PHOTOSYNTHETICA 38 (1): 111-126, 2000

Estimation of primary productivity by chlorophyll *a in vivo* fluorescence in freshwater phytoplankton

M. GILBERT, A. DOMIN, A. BECKER, and C. WILHELM*

Institute of Botany, Department of Plant Physiology, University of Leipzig, Johannisallee 19-23, D-04103 Leipzig, Germany

Abstract

Primary productivity in marine waters is widely estimated by the measurements of ^{14}C incorporation, the underwater light climate, and the absorption spectra of phytoplankton. In bio-optical models the quantum efficiency of carbon fixation derived from ^{14}C incorporation rates, the photosynthetically absorbed radiation derived from the underwater light climate, and the phytoplankton absorption spectra are used to calculate time- and depth-integrated primary productivity. Due to the increased sensitivity of commercially available fluorometers, chlorophyll *a in vivo* fluorescence became a new tool to assess the photosynthetic activity of phytoplankton. Since fluorescence data yield only relative photosynthetic electron transport rates, a direct conversion into absolute carbon fixation rates is not possible. Here, we report a procedure how this problem can be adressed in freshwater phytoplankton. We adapted a marine bio-optical model to the freshwater situation and tested if this model yields realistic results when applied to a hypertrophic freshwater reservoir. Comparison of primary productivity derived from ^{14}C incorporation to primary productivity derived from Chl a fluorescence showed that the conversion of fluorescence data into carbon fixation rates is still an unsolved problem. Absolute electron transport rates calculated from fluorescence data tend to overestimate primary production. We propose that the observed differences are caused mainly by neglecting the package effect of pigments in phytoplankton cells and by non-carbon related electron flow (*e.g.*, nitrogen fixation). On the other hand, the ^{14}C incorporation rates can be artificially influenced by "bottle effects", especially near the water surface, where photoinhibition, photorespiration, and Mehler reaction can play a major role.

Additional key words: absorption; bio-optical modelling; pigments; quantum yield; water quality.

Introduction

Control of water quality plays an increasing role in the responsibility of environmental protection agencies. In the past, water quality was mainly assessed by chemical and physical parameters. However, the intensified use of lakes or reservoirs for recreational activities as well as the growing awareness of water being a limited natural resource has increased the demand for surveillance of water quality on the biological level. Recent data sets focus more and more not only on the biomass but also on the population dynamics of organisms in the pelagial and in the benthos. On this background new technologies have been developed to assess quantitatively the

Received 14 June 1999, *accepted* 30 December 1999.
*Author for correspondence; fax: 49-341-9736899, e-mail: cwilhelm@rz.uni-leipzig.de
Abbreviations: CCM - carbon concentrating mechanism; Chl - chlorophyll; DIC - dissolved inorganic carbon; DOC - dissolved organic carbon; ETR - electron transport rate; fluorescence parameters for *dark-adapted state*: F_0 and F_m - fluorescence emission levels measured with Q_A oxidized or reduced, respectively; F_v - variable fluorescence (F_m - F_0); maximal Φ_{PS2} - maximal photosystem 2 quantum yield (maximal $\Phi_{PS2} = F_v/F_m$); fluorescence parameters for *operational state (under actinic irradiation)*: F - actual fluorescence intensity; F'_m - maximal fluorescence emission in the light adapted state; operational $\Phi_{PS2} = (F'_m - F)/F'_m$; HPLC - High Performance Liquid Chromatography; PAM - pulse amplitude modulated fluorescence; PAR - photosynthetically available radiation; *P-I* - photosynthesis-irradiance; POC - particulate organic carbon; PP - primary production; PS - photosystem; Q_{10} - temperature coefficient; TIC - total inorganic carbon. See also Table 1.
Acknowledgements: The research has been supported by the German Ministery of Education and Research (BMBF), grant no 02WU960/6.

phytoplankton composition by means of flow-cytometry (Phinney and Cucci 1989), HPLC-fingerprinting (Nixdorf and Hoeg 1993, Wilhelm *et al.* 1995, Wilhelm and Lohmann 1997), and spectroscopic methods (Yentsch and Phinney 1985, Beutler *et al.* 1998). In a near future an identification and quantification of species will be possible by means of molecular biology on the basis of *in situ* hybridisation and subsequent flow-cytometric analysis (Lange *et al.* 1996). With the help of these methods we understand better the fittings of organisms in aquatic ecosystems, but their activity is still hard to quantify. This statement is still valid if one takes into account modern approaches to measure growth rates under *in situ* conditions with the help of flow-cytometric cell counting or by determination of turn-over rates of taxon-specific pigments (Cailliau *et al.* 1996). The best parameter to assess the actual growth potential of a phytoplankton assemblage is the determination of the primary production, based on carbon incorporation.

Since the application of radioisotopes is legally restricted, especially for drinking water reservoirs, ^{14}C-based primary production measurements are not suitable for routine surveillance of inshore waters. Furthermore, until nowadays it is under debate if the ^{14}C-method measures gross or net primary production. A direct measurement of the gross primary production is probably impossible because the contribution of algal respiration to total respiration can not be assessed (Li 1993, Maestrini *et al.* 1993). Another restriction of this method is caused by the so-called "bottle effect" which alters the physiological activity of enclosed phytoplankton in an undefined way. Hence, an extrapolation of results from bottles to water column is difficult (Fitzwater *et al.* 1982, Williams and Robertson 1989), especially under high pH conditions occurring very often at the surface of freshwaters in summer time. The alternative method, *i.e.*, to measure oxygen production, is only rarely used due to the limited sensitivity which allows the application only in eutrophic or hypertrophic waters in Chl-rich layers (Williams and Jenkinson 1982).

Development of pulse-amplitude modulated (PAM) fluorometers which allow the measurement of photosynthetic quantum yields opens non-invasive possibilities to measure photosynthetic electron flow (Schreiber *et al.* 1995b). Together with recent progress in data processing capabilities and increased sensitivities of photodiodes this technology became applicable to phytoplankton measurements *in situ* (Schreiber *et al.* 1993, Trtilek *et al.* 1997, Kolber *et al.* 1998). However, the calculation of photosynthetic electron flow from photosynthetic quantum yields and incident radiant fluxes deliver only relative results which can not be easily converted to absolute values of primary production, *e.g.*, to mg(C fixed) m^{-2} d^{-1}. In order to assess the oxygen demand to mineralize the yearly produced organic matter, one of the most important parameters for long-term water quality in a given freshwater system, the carbon fluxes have to be known not only on the basis of relative photosynthetic activities but as absolute carbon fixation values. In this paper we present a first trial to convert fluorescence values together with irradiance and pigment measurements into maximum carbon quantum yields and oxygen evolution rates for a water reservoir under renovation and discuss problems which have to be solved in future.

For the estimation of primary production we applied different methods in parallel to identify problems and putative sources of errors. Apart from ^{14}C-incorporation rates we have calculated maximum quantum efficiencies of carbon fixation on the basis of fluorescence-based *P-I* curves and photosynthetically absorbed radiation (Q_{phar}). The latter was calculated from the *in situ* irradiance at a given depth and the corresponding absorption spectrum of the phytoplankton cells reconstructed by using the volume-based concentration of phytoplankton pigments. The same data set was used to calculate theoretical oxygen evolution rates. The results of these calculations were compared with results from literature to test the validity of the model and to identify those parameters which may be the most important sources of errors leading to strong misestimates of primary production.

Materials and methods

Sampling site: The "Bleilochtalsperre" in Thuringia (50°30′N, 11°42′E), with a volume of 215 km^3 and a surface area of 9.2 km^2 is one of the biggest dams in Germany. Due to sewage waters and extensive agriculture it is in a hypertrophic state with a high risk of algal blooms. Industrial effluents of a paper mill with a high concentration of gilvin are responsible for the dark brown colour of the water and a photic layer of less than 2 m on an average depending on the phytoplankton concentration as well. Due to the absorption of gilvin, the blue and blue-green parts of the spectrum are dwindling very fast with increasing depth. The vertical attenuation coefficient K_d (related to PAR) varies between 2.5 and 3.0 m^{-1}. Almost no quanta of wavelengths between 400 and 550 nm can penetrate to the depth of 2 m (values not shown). Near the dam wall a jet pipeline for compressed air is installed at 25 m depth for destratification of the water column. The

induced circulatory current drifts phytoplankton cells from the surface to the aphotic zone to reduce primary production. The experimental site, called 'Piere', is located about 10 km from the dam wall. It was chosen for this study because it is enough distant from the destratification system to develop a well stratified water column. This is an important prerequisite to compare photosynthetic rates obtained from ^{14}C-incorporation in statically exposed bottles with those calculated from fluorescence measurements.

HPLC analysis: Glass-fibre filters (*GF6, Schleicher & Schüll*, Dassel, FRG) with filtered phytoplankton samples were frozen immediately in liquid nitrogen, freeze-dried in the laboratory, and stored at –35 °C. For pigment extraction the filters were homogenized in solvent [0.5 M ammonium acetate/methanol : H_2O : ethylacetate, 77 : 14 : 9 (v:v:v)] and a mixture of glass beads [0.25-0.3 mm : 1-1.05 mm, 1 : 3 (v:v)] for 30 s under dry ice cooling using a cell homogenizer (*Braun*, Melsungen, FRG). Insoluble fragments were removed by centrifugation at 5000×*g* (30 s). The injection volume varied between 30 and 300 mm^3 depending on the Chl content. Pigment concentrations of the samples were calculated from the areas of peaks, using the calibration described in Wilhelm *et al.* (1995) and the ratio of injected/filtered volume.

HPLC-analysis was performed with a Waters Chromatography System, including a photodiode array detector, an autosampler, and a *Millennium* software (vers. *2.0*). For the separation a reversed phase system was used, with a *Nucleosil* wide pore C18-5 µm, 30 nm (250×8×4 mm) column and a ternary gradient of the solvents A [0.5 M ammonium acetate/methanol : H_2O, 85:15 (v:v)], B [acetonitrile : H_2O, 90 : 10 (v : v)] and C (100 % ethylacetate), running 32 min at a flow rate of 13.33 $mm^3\ s^{-1}$ (0 min: 60 % A, 40 % B; 2 min: 100 % B; 7 min: 80 % B, 20 % C; 17 min: 50 % B, 50 % C; 21 min: 30 % B, 70 % C; 29.5 min: 30 % B, 70 % C; 31 min: 30 % A, 70 % B; 32 min: 60 % A, 40 % B). The detection wavelengths for integration were set to 440 nm (all carotenoids and Chls) and to 670 nm (Chl *a* and its degradation products), additionally on-line spectra from 350-750 nm (resolution 1.2 nm) were recorded every second. During analysis the column temperature was kept constant at 18-20 °C, leading to pressures between 11.030 and 12.755 MPa.

The contribution of different algal groups in phytoplankton assemblages to total Chl *a* was calculated from the amounts of the biomarker pigments peridinin (*Dinophyta*), fucoxanthin (*Bacillariophyceae* and *Chrysophyta*), alloxanthin (*Cryptophyta*), lutein or Chl *b* (*Chlorophyta*), and zeaxanthin (*Cyanobacteria*), using laboratory references (Wilhelm *et al.* 1995) which were modified in an iterative way (models were compared to statistical multivariate regressions). Because of the relatively high amount of samples and their rather good homogeneity, highly significant models were found to quantify at least the percentage contribution of the major groups (*Chlorophyta, Bacillariophyceae, Cryptophyta*).

Calculation of photosynthetically absorbed radiation (Q_{phar}): Photosynthetically absorbed radiation was calculated from reconstructed phytoplankton absorption spectra and measurements of the underwater radiation field. Phytoplankton absorption spectra were reconstructed according to Bidigare *et al.* (1990) from the *in vivo* weight-specific absorption coefficients of the major pigment groups and their volume-based concentrations using the HPLC data set of pigments [Eq. (1), cf. Table 2]. "Pigment package" effects, which vary with intracellular pigment concentration and cell size, were not taken into account when reconstructing the absorption spectra. The following pigments were not included in the reconstruction of absorption spectra: β-carotene (since quantitative extraction was not assured) and the water-soluble phycobiliproteins. The underwater radiation field (downwelling irradiance) was measured by a *LI-COR 1800* underwater spectroradiometer (*LI-COR*, Lincoln, USA) at wavelength-steps of 1 nm. Integrated Q_{phar} was computed using Eq. (2). We modified the approximate forms of equations, used widely in marine research (*e.g.*, Smith *et al.* 1989, Eq. 2), into their explicit versions based on the Lambert-Beer law. At Chl *a* concentrations of several mg m^{-3} up to 250 mg m^{-3} as found in the investigated water reservoir the approximation of $\ln(1 - A) \approx A$ (if $A \ll 1$) is no longer valid. Corrections of Q_{phar} concerning the absorption of non-photosynthetic pigments were only applied for the theoretical computation of O_2 evolution rates (see below).

PAM-fluorescence-measurements: Samples were taken every month from March until September and at 14 d intervals in July and August 1998 in the stratified water column at the site 'Piere' with a 5 000 cm^3 Ruttner-sampler (*Hydro-Bios*, Kiel, FRG). Samples were prefiltered through a 0.5 mm mesh in order to remove larger zooplankton. The Xenon-PAM-fluorometer (*Walz*, Effeltrich, FRG) was used in connection with the *ED101-US*-cuvette holder and a standard 10×10×45 mm quartz cuvette mirrored at one side (Schreiber *et al.* 1993, Schreiber 1994). Additionally, the set-up was supplemented with a home-made temperature control and a stirrer which was essential to avoid artificial changes in P_{max} determinations. The samples were measured without any pre-concentration procedure at 20 °C. Excitation radiation (*EG&G, FX134*) was filtered through a *BG39* filter (λ = 400-560 nm, *Schott*, Mainz,

FRG). Fluorescence emission was separated from scattering radiation of the measuring beam by *GG10* and *RG 645* filters ($\lambda > 650$ nm, *Schott*, Mainz, FRG). Fluorescence nomenclature is used according to van Kooten and Snel (1990). Dark-adapted maximum quantum efficiency F_v/F_m was determined after 5 min dark adaptation and the operational quantum yield $\Delta F/F'_m$ (Genty *et al.* 1989) after 90 s of light-adaptation at successively increasing irradiances (6, 12, 18, 96, 480, 655, 980, and 1460 µmol m^{-2} s^{-1}). Values were corrected by subtracting fluorescence (gilvin, filters, and scattering of excitation radiation) of filtered water samples (*GF6*, *Schleicher & Schüll*, Dassel, FRG). The actinic irradiance (Q_0, PAR) in the cuvette was measured with a spherical 4π sensor (*Zemoko*, Koudekerke, NL) of 8 mm diameter. Adjustment of actinic irradiances by neutral density filters (*Schott*, Mainz, Germany) and electronic dimming of the halogen light source resulted in small spectral differences. Photosynthetically absorbed radiation Q_{phar} was calculated (see above) in consideration of these spectral differences by measuring the spectral emission characteristics of the actinic radiation source at each intensity setting with a spectroradiometer. Photosystem 2 (PS2) electron transport rates were calculated as the product of Φ_{PS2} and $Q_{phar}/2$ and fitted by the photosynthesis model from Eilers and Peeters (1988) according to Eq. (3). We also tested *P-I* models described by Gallegos and Platt (1981), Neale and Richerson (1987), and Walsby (1997). The model of Eilers and Peeters (1988) was used to fit all the data, because it described at best the data points in the overall cases (*e.g.*, with and without photoinhibition). Furthermore, it did not result in strong overestimated fit values of P_{max} compared to actual P_{max} values derived from the PAR-saturated part of the curves.

^{14}C-measurements: Radiocarbon measurements were done on 8 and 22 July, and 5 and 19 August in 250 cm^3 glass bottles horizontally adjusted in 0 (only in August), 0.2, 0.5, 1, and 2 m with 0.37 MBq $NaH^{14}CO_3$ per bottle from 12:00-15:00 h. Total radioactivity of the tracer was measured by counting 1 cm^3 tracer solution in 5 cm^3 *HionicFluor* (*Canberra Packard*, Meriden, USA) + 300 mm^3 ethanolamine + 1 cm^3 ethylene glycolmonomethylether (*Merck*, Darmstadt, FRG). Incorporation was stopped by adding 1 cm^3 formalin (36 %) per bottle. Triplicates (75 cm^3) of each bottle were filtered on *GF6*-filters (Ø 25 mm, *Schleicher & Schüll*, Dassel, FRG) in the laboratory. Filters were transferred onto 0.5 M HCl soaked paper for 10 min and afterwards onto 0.5 M NaOH soaked paper to exclude inorganic tracer. Radioactivity was measured in 20 cm^3 glass vials (*Beckman Instruments*, Fullerton, USA) in a *1409-LSC*-Counter (Wallac Oy, Finland) for 3 min in 10 cm^3 *OptiPhase SuperMix* (Wallac Oy, Finland) using the external standards ratio method to correct for quenching. The ^{14}C-incorporation in the bottles was corrected by the dark bottle values. Q_0 (PAR) was recorded continuously during incubation at 0 m using a *LI-190SA* quantum sensor (*LI-COR*, Lincoln, USA). Q_0 at other depths was calculated using attenuation coefficients derived from underwater spectro-radiometer measurements. Total inorganic carbon (TIC) was measured according to Deutsche Einheitsverfahren zur Wasseruntersuchung (1995).

Computing maximum quantum efficiencies of carbon fixation (Φ^C_{max}): Since ^{14}C based *P-I* curves were not measured we used the model of Smith *et al.* (1989) to calculate the maximum quantum yield of carbon fixation. The mathematical structure of this model describes a Michaelis-Menten saturation kinetics based on the spectrally independent model of Kiefer and Mitchell (1983). Smith *et al.* (1989) derived a spectrally dependent form of this model where quantum yield can vary as a function of I_k and with depth, Eq. (4). For computation of Φ^C_{max} the I_k values derived from variable fluorescence-based *P-I* curve fits [Eq. (3)] were used. The spectrally weighted phytoplankton absorption coefficient $\bar{a}_{ph}$ was calculated according to Eq. (5). We used the explicit version of this equation instead of the approximate form (*e.g.*, Kroon *et al.* 1993, Eq. 1) due to the same reasons as described for the calculation of Q_{phar}.

Calculation of theoretical oxygen evolution rates: No measurements of oxygen evolution were performed. Hence, the computation of theoretical oxygen evolution rates was carried out by using the experimental variable fluorescence-based *P-I* values. The PS2 quantum yield, Φ_{PS2}, as a function of incident radiation was fitted by the dynamic phytoplankton photosynthesis model according to Eilers and Peeters (1988), Eq. (3). The resulting parametrisation of the experimental values allowed to calculate Φ_{PS2} at every irradiance and to compute Φ_{PS2} for all actual irradiances at the field site using the laboratory PAM measurements and the underwater irradiance values from the water reservoir. To evolve 1 oxygen molecule in "ideal photosynthesis", four charge separations have to take place at PS2 and the four liberated electrons require the trapping of 4 photons at PS2 and 4 more photons at PS1. The maximum theoretical quantum yield for oxygen evolution is therefore 0.125 and the stoichiometric ratio of oxygen evolved per electron liberated at PS2 is 0.25. Assuming that the fraction of absorbed PAR which is transferred to PS2 is 0.5, the theoretical oxygen evolution rate is given by the product of $\Phi_{PS2} \times 0.25 \times 0.5 \times Q_{phar}$. Concomitant normalisation to Chl *a* will result in the theoretical Chl-based oxygen evolution rate at the respective depth.

Corrections for temperature were performed by multiplying the PAR-saturated O_2-evolution rates of surface samples (0 m) by the factor $Q_{10}^{(T\,in\,situ\,-\,Tlaboratory)/10}$. Since we did not measure the temperature dependence of photosynthesis, Q_{10} was set at 2.0 (Walsby 1997). $T_{laboratory}$ was set at 20 °C, the temperature of fluorescence measurements.

A major problem for the calculation of theoretical O_2 evolution rates is the absorption by non-photosynthetic pigments. To investigate the influence of this photosynthetically inefficient absorption capacity on the theoretically derived O_2 rates, we corrected the reconstructed absorbance spectra by two different procedures: According to Schofield *et al.* (1996) the absorption of photoprotective pigments was subtracted from the overall absorption spectra, concerning the pigments alloxanthin, lutein, diadinoxanthin, and zeaxanthin ($Q_{phar}2$). A second procedure ($Q_{phar}3$) was based on the computation of corrected absorbance spectra using the ratio of absorbance to fluorescence excitation spectra digitized from data in literature (Culver and Perry 1999).

Table 1. Symbols.

$Q_0(\lambda, z)$	Photosynthetically available radiation at depth z [µmol m^{-2} nm^{-1} s^{-1}]
$Q_{phar}(z)$	Photosynthetically absorbed radiation at depth z [µmol m^{-2} s^{-1}]; [µmol m^{-3} s^{-1}], if Δz = 1 m
$Q_{phar3hmean}(z)$	Photosynthetically absorbed radiation at depth z averaged for the 3 h incubation period during ^{14}C incorporation [µmol m^{-2} s^{-1}]; [µmol m^{-3} s^{-1}], if Δz = 1 m
$a_i(\lambda)$	Pigment-specific *in vivo* absorption coefficients for the major absorbing pigment groups at wavelength λ [m^2 mg^{-1}]
$a_{ph}(\lambda,z)$	Reconstructed chlorophyll *a* specific *in vivo* absorption coefficient of the phytoplankton sample at wavelength λ [m^2 mg^{-1}(Chl*a*)]
$C_i(z)$	Pigment concentration at depth z [mg(pigment) m^{-3}]
[Chl*a*]	Chlorophyll *a* concentration at depth z [mg(Chl*a*) m^{-3}]
λ	Wavelength [nm]
z	Depth [m]
Δz	Pathlength through phytoplankton containing layer [m]
P	Rate of photosynthesis [mmol(C) kg^{-1}(Chl*a*) s^{-1}] or [mmol(e^-) kg^{-1}(Chl*a*) s^{-1}]
P_{max}	Maximum rate of photosynthesis [mmol(C) kg^{-1}(Chl*a*) s^{-1}] or [mmol(e^-) kg^{-1}(Chl*a*) s^{-1}]
I	Integrated photosynthetically available radiation from 400-700 nm (PAR = Q_0)[µmol m^{-2} s^{-1}]
I_k	*P-I* saturation parameter ($I_k = P_{max}/\alpha$) [µmol m^{-2} s^{-1}]
α	Initial slope of the *P-I* curve [mmol(C) kg^{-1}(Chla) s^{-1} (µmol m^{-2} s^{-1})$^{-1}$] or [mmol(e^-) kg^{-1}(Chla) s^{-1} (µmol m^{-2} s^{-1})$^{-1}$]
Φ^C	Quantum efficiency for carbon fixation [mol(C) mol^{-1}(quanta absorbed)] or [mol(C) mol^{-1}(e^-)]
Φ^C_{max}	Maximum quantum efficiency for carbon fixation [mol(C) mol^{-1}(quanta absorbed)] or [mol(C) mol^{-1}(e^-)]
$\bar{a}_{ph}(z)$	Spectrally weighted absorption coefficient of phytoplankton at depth z [m^{-1}]
$\bar{A}(z)$	Spectrally weighted absorptance of phytoplankton at depth z

Results and discussion

Distribution of algal classes: The phytoplankton concentration at the sampling site 'Piere' changed during the vegetation period showing blooms in April, June, July, and late August with clear water periods in between. Changes in Chl *a* were accompanied by variations in algal composition, especially on two days in May, when heavy rainfall increased the water volume of the reservoir and led to a decrease in the percentage distribution of diatoms and chlorophytes and a percentage increase of cryptophytes (Fig. 1). One month later the former phytoplankton composition was nearly restored. On the average (0-2 m, n = 106) the site was dominated by diatoms (43 %) followed by *Chlorophyta* (35 %) and *Cryptophyta* (19 %), but only minor amounts of *Cyanobacteria* and *Dinophyta* were observed. Comparing the phytoplankton on 27 May and 23 June, the Chl *a* concentration differed by a factor of 15 and the phytoplankton composition showed large variations. These changes in biomass amount and composition strongly affected the *in situ* irradiance climate and hence,

Table 2. Equations.

$a_{ph}(\lambda, z) = \frac{\sum_{i=1}^{n} a_i(\lambda, z) C_i(z)}{[Chl\ a]}$	(1)
$Q_{phar}(z) = \int_{400nm}^{700nm} Q_0(\lambda, z) - Q_0(\lambda, z) \times e^{-a_{ph}(\lambda, z)[Chl\ a]\Delta z}\, d\lambda$	(2)
$P = \frac{I}{aI^2 + bI + c}$; $\alpha = 1/c$; $P_{max} = 1/(b + 2\sqrt{ac})$; $I_k = c/(b + 2\sqrt{ac})$	(3)
$\frac{\Phi(z)}{\Phi_{max}} = \frac{I_k \times \bar{a}_{ph} \times [Chl\ a]}{I_k \times \bar{a}_{ph} \times [Chl\ a] + Q_{phar}}$	(4)
$\bar{a}_{ph} = -1/\Delta z \times \ln(1 - \bar{A})$; $\bar{A} = \frac{\int_{400}^{700} Q_{phar}(\lambda, z)\, d\lambda}{\int_{400}^{700} Q_0(\lambda, z)\, d\lambda}$	(5)

P-I curves measured *ex situ* by non-diving fluorometers could not be used directly to describe photosynthetic efficiency of the cells *in situ*. Therefore, we tried to estimate the Q_{phar} *in situ*.

Calculation of Q_{phar} is a prerequisite to estimate theoretically derived O_2 evolution rates and operational carbon-based quantum yields from ^{14}C incorporation. Fig. 2 presents some selected spectra of Q_{phar} in the wavelength range 400-700 nm at Chl *a* concentrations of 30 and 100 mg m^{-3}. Significant deviations in the integrated Q_{phar} occurred already at low Chl *a* concentrations (Fig. 2, *insert*). A Chl *a* concentration of 5-10 mg m^{-3} results in an overestimation of the integrated Q_{phar} by 5-10 % when applying the approximate version (cf. Eq. 2, Smith *et al.* 1989) as compared to the explicit form described by Eq. 2 (cf. Table 2). Deviations at different wavelengths varied due to those differently calculated absorption coefficients and/or number of pigment-classes absorbing at the same wavelength band. Already the sample with a Chl *a* concentration of 30 mg m^{-3} showed a strong deviation in the Soret band leading to a higher Q_{phar} than Q_0 in this wavelength band which is physically impossible. At Chl *a* concentrations of 100 mg m^{-3}, often observed in lake Bleiloch (Fig. 1), the integral of Q_{phar} exceeds even that of incident irradiance Q_0, an obvious artefact, since the absorbed radiation can never exceed the total incident PAR. The spectra show that the ratio of absorbed/incident PAR changes drastically as a function of depth, wavelength, and the time of sampling, *i.e.*, the amount of biomass and phytoplankton composition. As a conclusion from this result we have plotted *P-I* curves from fluorescence measurements not as a function of incident PAR but as a function of Q_{phar}.

PAM-fluorescence-measurements: Variable fluorescence was measured in samples down to Chl *a* concentrations of 5 mg m^{-3}. During the vegetation period operational and maximum quantum yields did not differ significantly between samples taken from 0-2 m ($p<0,05$, Student's *t*-test, $n = 45$, values not shown), although the sampling site 'Piere' showed a well stratified water column with the possibility of photoadaptation of phytoplankton. However, photoacclimation obviously did not play a significant role at site 'Piere' (Fig. 3). The initial slopes of the *P-I* curves were almost identical and there was no clear dependence of P_{max} on water depth. The samples taken from the surface and from 2 m depth show very similar P_{max} values, while the sample from 1 m depth shows a slightly smaller P_{max} value and higher sensitivity to photoinhibition.

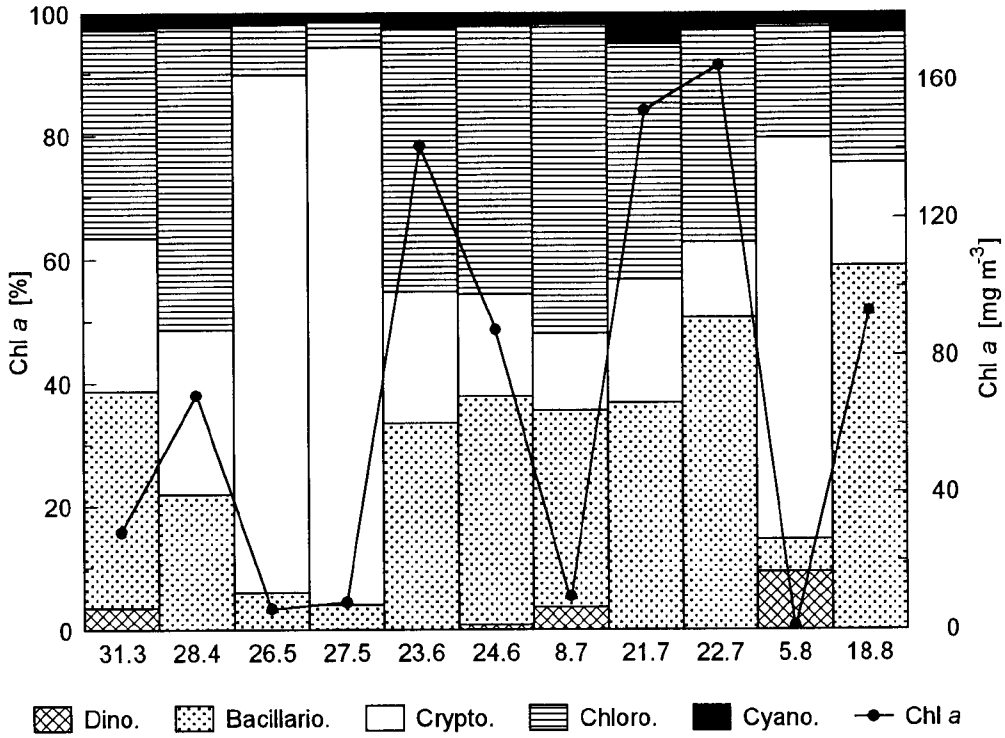

Fig. 1. Phytoplankton composition and chlorophyll (Chl) *a* concentration [mg m^{-3}] at sampling site 'Piere', 0 m, March-August 1998.

In order to test changes in physiological activity during the time of ^{14}C-incubation we measured fluorescence-based *P-I* curves before and after incubation of phytoplankton samples in sealed bottles for 3 h in parallel to the ^{14}C experiments. In Fig. 4 *P-I* curves are plotted from five different depths. The values after incubation were scaled to their corresponding values before incubation (100 %). Depending on depth, *i.e.*, solar irradiance over the period of incubation, maximum reductions in operational quantum yields and P_{max} (-34 %) were recorded in the 0 m sample, whereas the 2 m sample showed higher operational quantum yields and P_{max} (+23 %) after the exposition. The α-slope was reduced by 33 % in the 0 m sample and did not change significantly (according to variations of the fit model) in the 2 m sample (Table 3). These values are a strong support that inclusion of the phytoplankton cells in sealed bottles reduces their physiological activity the more the cells are exposed to high irradiances. The artificial nature of this reduction in photosynthetic activity is supported by the fact that the α-slopes in *P-I* curves from phytoplankton samples taken from different depths show no photoinhibitory effect before inclusion (Fig. 3).

^{14}C-measurements: Carbon-based primary production determinations showed pronounced reduction of carbon incorporation rates in the samples exposed at the surface compared to those at 0.2 m depth, where incident radiation was already reduced to 56 % of the 0 m value. On 5 August, the primary production at the surface was reduced by 29 % and on 19 August by 14 % on Chl *a* basis (Fig. 5, Table 4). The availability of total inorganic carbon (TIC) is not a convincing argument to explain these differences because the concentrations were too high to be limiting (Table 4).

The radiocarbon incorporation rates did not follow the irradiance (Fig. 5, *solid line without symbols*). Primary production decreased linearly with the depth whereas PAR dropped down exponentially. An exception were the values from 22 July when the vertical temperature and pH gradients were the most prominent and might have affected ^{14}C-incorporation rates. On 22 July, temperature decreased by 31 % from 24.5 to 16.9 °C and pH by 12 % from 9.3 to 8.2 (Table 4) within the first two meters, the average decrease in temperature was 4 % and 7 % for pH on the other days (Table 4). On 8 July, 5 August, and 19 August, carbon incorporation rates showed a linear-like pattern and did not follow the exponential decrease in incident PAR. This is in line with observations of Watanabe (1980) who studied excretion and extracellular products of natural

phytoplankton assemblages in the freshwater Lake Nakanuma (Japan) by means of ^{14}C-incorporation. In the eutrophic Lake Nakanuma Secchi-depth was 1-2 m, similar to 1.6 m (n = 13, std ±0.61) at sampling site 'Piere'. In these hypertrophic water bodies a steep reduction of ^{14}C-incorporation rates with depth may be expected, but was not observed. Kolber and Falkowski (1993) reported a reduction of ^{14}C-incorporation in bottles exposed near the surface compared to exposures at deeper layers in the north-west Atlantic Ocean. Although Chl *a* concentration was nearly constant and incident irradiance decreased exponentially, in contrast ^{14}C-incorporation did not. These findings may reflect the difficulties and problems associated with the ^{14}C-method and/or may be the result of, *e.g.*, photorespiration, different incorporation rates, and carbon concentration mechanisms (CCM) of algae at different depths. The existence of CCMs has been reported for all taxa contributing significantly to planktonic primary production in the ocean and in freshwaters (*e.g.*, *Cyanobacteria, Bacillariophyceae, Dinophyceae, Chlorophyceae,* and *Prymnesiophyceae*, see Raven 1991, Table 1). Excreted dissolved organic carbon (DOC) is thought to be usually less than 10 % of POC in healthy cells (see a critical review of Sharp 1977) but the amount of excreted products may be increased especially under high irradiance or under nutrient deficiency, and therefore may be a reason for the lower amount of $PO^{14}C$ in the surface samples (*e.g.*, Watanabe 1980, Baines and Pace 1991, Karl *et al.* 1998). Plotting a linear regression of ^{14}C primary production *versus* absorbed radiation on four days of exposition at the site 'Piere' resulted in a calculated quantum yield Φ^C of 0.011 mol(C) mol^{-1}(quanta absorbed) (Fig. 6), which is in accordance with values of other investigations in marine research (Table 5). This basic agreement with results from literature was taken as a basis to correlate measured carbon-based photosynthetic rates with PAM-measured electron transport rates.

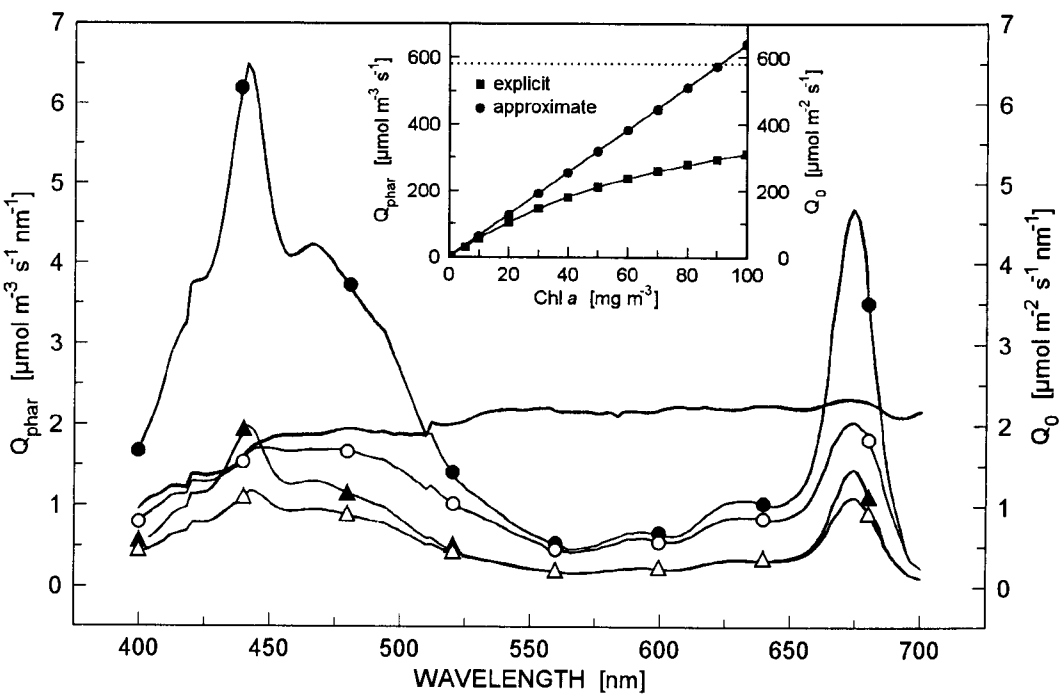

Fig. 2. Photosynthetically absorbed radiation (Q_{phar}) calculated from HPLC values and incident irradiance Q_0 at the surface for 30 mg(Chl *a*) m^{-3} (*triangles*) and 100 mg(Chl *a*) m^{-3} (*circles*). *Open symbols* represent calculations based on the explicit version of Eq. (2), *closed symbols* calculations based on the approximate form [*e.g.*, Smith *et al.* 1989, Eq. (2)]. The *solid line* without symbol shows the incident irradiance Q_0. *Insert*: Q_{phar} plotted as a function against the Chl *a* concentration. *Closed squares* represent the curve for the explicit form of Eq. (2), *closed circles* for the approximate computation. The integral of Q_0 (PAR) is given by the *horizontal dashed line*.

Correlation of ^{14}C-measurements with variable fluorescence data: Photosynthetic electron flow determinations on the basis of F_v measurements were correlated with oxygen or ^{14}C-uptake by several authors with different results. Although mostly used for higher plants, some researchers have applied fluorescence techniques also to unicellular algae and phytoplankton (*e.g.*, "Pump and Probe": Falkowski *et al.* 1986, Kolber

and Falkowski 1993, Boyd *et al.* 1997; LED-PAM: Rees *et al.* 1992, Hofstraat *et al.* 1994, Hartig and Coljin 1996, Geel *et al.* 1997, Hartig *et al.* 1998). Although the investigations were conducted under a variety of experimental conditions, a linear correlation between oxygen evolution and PS2-related electron flow was found under moderate irradiances, with varying α-slopes for different algal species. Non-linear correlations were observed under high irradiances (Falkowski *et al.* 1986, Rees *et al.* 1992) and in some cases under low irradiances (Falkowski *et al.* 1986, Schreiber *et al.* 1995a, Hartig *et al.* 1998). For these deviations different explanations are proposed: spectral differences in PAR sources, changes in oxygen consumption in the light, inactive PS2 centres, cyclic electron flow around PS2, and Mehler reaction.

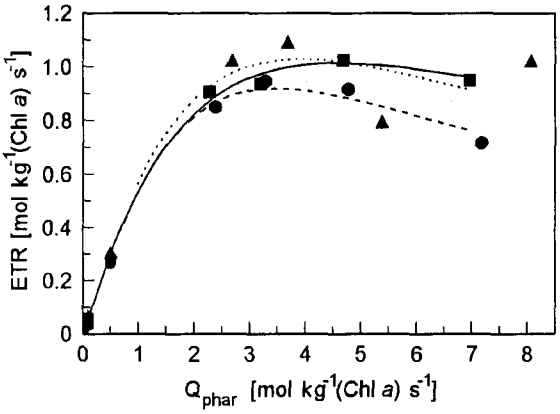

Fig. 3. Photosystem 2 (PS2)-related electron transport rates normalized to chlorophyll (Chl) *a* on 19 August 1998, at 0 m (*squares*), 1 m (*circles*), or 2 m (*triangles*). *Lines* show fit-curves according to photosynthesis model of Eilers and Peeters (1988), Eq. (3).

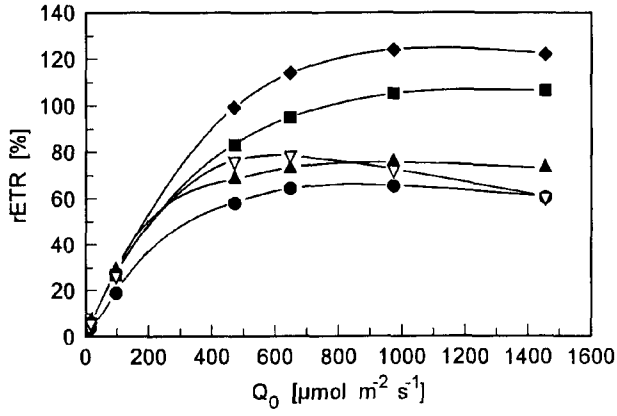

Fig. 4. Relative electron transport rates of phytoplankton exposed in static glass bottles for 3 h at 0 m (*circles*), 0.2 m (*solid triangles*), 0.5 m (*open triangles*), 1 m (*squares*), and 2 m (*diamonds*). Percentage of value before incubation (100 %) at corresponding depth and irradiance.

When PS2-related electron flow is correlated with the radiocarbon-incorporation *in situ*, the bottle effect on phytoplankton activity has to be taken into account. As shown in Fig. 4, in bottles exposed at the surface artificial depression of photosynthesis is observed. This leads to three questions: First, is there a similar change of the operational quantum yield in samples that were not incubated in glass bottles? Second, which operational quantum yield (at the beginning, intermediate, at the end, or mean over the whole period of time, Fig. 4) should be correlated to the ^{14}C-based quantum yield? And third, which Q_{phar} value should be used when computing ETR and carbon quantum yields? Since the radiocarbon-measurement is a time-integrating method we computed ETR from Q_{phar} values averaged over 3 h periods of incubation. To quantify the putative bottle effect we used the operational quantum yields (Φ_{PS2}) before and after incubation. Due to the reduction of the operational quantum yields during the bottle incubation, mean fluorescence-based Φ^C values derived from linear

Table 3. Parameters of *P-I* curves α [relative], I_k [µmol m^{-2} s^{-1}], and P_{max} [relative] on 19 August 1998 fitted according to photosynthesis model of Eilers and Peeters (1988). The curves were generated by plotting relative ETR ($\Phi_{PS2} \times Q_0$) *versus* Q_0 before (*ante*) and after (*post*) 3 h incubation in statically exposed glass bottles. Percentage of value before incubation is given in column *post/ante*.

Depth [m]	ante			post			post/ante		
	α	I_k	P_{max}	α	I_k	P_{max}	α	I_k	P_{max}
0.0	0.69	299	207	0.46	293	136	67	98	66
0.2	0.64	319	203	0.75	203	151	117	64	75
0.5	0.66	289	192	0.62	247	153	93	86	80
1.0	0.66	276	181	0.65	283	184	99	102	102
2.0	0.80	225	181	0.76	293	223	94	130	123

regression changed from 0.057 to 0.074 mol(C) $mol^{-1}(e^-)$ (Fig. 7). This result shows the problem to scale up the results from fast measurement techniques such as the PAM-fluorescence-method (or even faster ones like the pump and probe method, see above) with slow time-integrating ones such as the radiocarbon method.

Table 4. ^{14}C primary production (PP) [mmol kg^{-1}(Chl) s^{-1}] or [mg m^{-3} per 3 h], chlorophyll (Chl) *a* concentrations [mg m^{-3}], total inorganic carbon (TIC) [g m^{-3}], and physico-chemical parameters.

Date	Depth [m]	PP per Chl	PP 3 h	Chl *a*	TIC	Temp. [°C]	pH
8 July	0.2	37	47	9.8	19.8	16.2	8.7
	0.5	24	30	9.8	19.6	16.2	8.3
	1.0	17	20	9.0	19.7	16.1	8.1
	2.0	3	4	9.2	19.8	16.1	7.8
22 July	0.2	34	717	164.2	16.2	24.5	9.3
	0.5	12	272	174.8	13.8	22.1	9.2
	1.0	2	39	191.1	10.2	20.4	8.7
	2.0	1	15	108.4	14.4	16.9	8.2
5 August	0.0	72	17	1.8	19.2	20.4	7.8
	0.2	100	24	1.8	20.4	20.3	7.7
	0.5	67	19	2.1	19.6	20.3	7.6
	1.0	46	10	1.6	19.7	19.9	7.5
	2.0	11	3	1.8	19.2	19.7	7.4
19 August	0.0	19	222	87.6	15.6	21.1	9.5
	0.2	23	255	87.6	15.8	21.0	9.4
	0.5	17	192	88.1	16.2	21.0	9.4
	1.0	11	119	81.6	16.3	20.8	9.3
	2.0	1	9	58.7	16.5	19.6	8.9

Maximum quantum efficiencies of carbon fixation: In Table 6 we have listed the spectrally weighted absorption coefficient (Eq. 5), the PAR saturation coefficient I_k (from the fit of PAM-measured *P-I* curves according to Eq. 3), the effective quantum efficiency of carbon fixation (^{14}C-incorporation rate divided by Q_{phar}), and the maximum quantum efficiency of carbon fixation (Eq. 4).

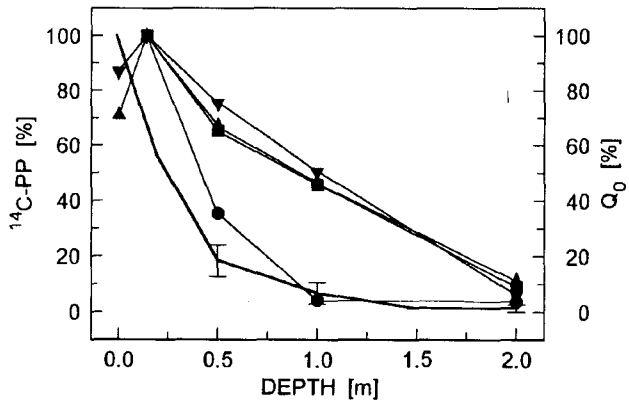

Fig. 5. Vertical profiles of ^{14}C primary production in 1998 (*squares* 8 July; *circles* 22 July; *up triangles* 5 August; *down triangles* 19 August) and incident irradiance Q_0 [% of value at 0 m] (*solid line without symbols*, n = 11).

Due to the fact that the I_k determination depends strongly on the fit model and therefore *P-I* curves with a standard error of 15 % can produce changes in I_k of a factor of two (Wilhelm and Wild 1984), we have tested the influence on I_k-variations. In the case of $\Phi^C{}_{max}{}^*$, I_k was multiplied by 0.5 and in the case of $\Phi^C{}_{max}{}^{**}$, I_k was doubled. The calculated $\Phi^C{}_{max}$ values are ranging from 0.011 to 0.079 mol(C) mol^{-1}(quanta absorbed) (Table 6), and are in good agreement with a study on marine microphytobenthic algae (Hartig *et al.* 1998, Table 3), where $\Phi^C{}_{max}$ values derived from measured ^{14}C-based PI curves varied between 0.018 to 0.077 mol(C) mol^{-1}(quanta). In general, we found very good agreement between measured and calculated quantum yields under PAR limitation, but less coincidence under PAR saturation or photoinhibiton. The most consistent pattern of measured Φ^C was shown by the values from 19 August (Table 6). Φ^C increased steadily with depth and with decreasing irradiance Q_0 from PAR-saturated to PAR-limited photosynthesis. The calculated $\Phi^C{}_{max}$ values are considerably higher than the operational quantum yields Φ^C marked by a declining difference between each other with increasing depth as can be expected from theory (0 m: Φ^C = 27 % of $\Phi^C{}_{max}$, 0.5 m: 69 %, 1 m: 88 %, 2 m: 98 %). At 2 m depth there

Table 5. Maximum (Φ^C_{max}) and operational (Φ^C) quantum yields and minimum ($1/\Phi^C_{max}$) and operational ($1/\Phi^C$) photon requirements of ^{14}C fixation, for Schofield *et al.* (1991, 1996), Kroon *et al.* (1993), Hartig *et al.* (1998), and Moisan and Mitchell (1999) depending on irradiation of culture.

	Irradiation	Φ^C_{max}	$1/\Phi^C_{max}$
Hartig *et al.* (1998)	halogen	0.018-0.077	13-56
Schofield *et al.* (1996)	blue	0.04	25
	green	0.06	17
	red	0.02	50
Kroon *et al.* (1993)	blue	0.015	66
	green	0.024	42
	red	0.014	71
Schofield *et al.* (1991)	blue	0.04-0.20	5-25
	green	0.01-0.03	33-100
	red	0.010-0.055	18-100
		Φ^C	$1/\Phi^C$
our data	*in situ*	0.011	89
Moisan and Mitchell (1999)	blue	0.003-0.090	11-333
Kroon *et al.* (1993)	blue	0.007	143
	green	0.022	45
	red	0.004	250

is almost no difference between operational and maximum quantum yield.

A major problem is the use of fluorescence-based I_k values. I_k values derived from variable fluorescence, O_2 evolution, and ^{14}C fixation measurements can differ significantly from each other. For *Heterocapsa pygmaea* the I_k values of C fixation, depending on the spectral quality of PAR, are 2-3 times larger than the oxygen-based I_k values, while fluorescence-based values are in good agreement with the oxygen-based ones (Kroon *et al.* 1993). Nevertheless, Hartig *et al.* (1998) observed about a twofold increase of I_k values measured by variable fluorescence compared to ^{14}C based measurements. Since Φ^C/Φ^C_{max} are non-linearly determined by I_k, $\bar{a}_{ph}$, and Q_{phar} according to Eq. (4) we tested the influence of the I_k parameter relative to its effect on the calculated value of Φ^C_{max}. For this purpose we multiplied or divided the fluorescence-based I_k values by a factor of 2 and calculated the new Φ^C_{max} values according to Eq. (4). The absolute Φ^C_{max} values changed considerably, increasing between 2 and 70 % in case of I_k being half of the fluorescence-based value and decreasing between 1 and 35 % in case of doubling its value. However, the above observed variation of Φ^C_{max} values with depth (Table 6) can not be explained only by changes in I_k and Q_{phar} [cf. Eq. (4)]. Since each phytoplankton sample was taken from its respective depth and exposed at the same depth during the bottle experiments, each Φ^C_{max} value may also represent the adaptation to the strongly varying spectral distribution of PAR at different depth (cf. Materials and methods, "Sampling site").

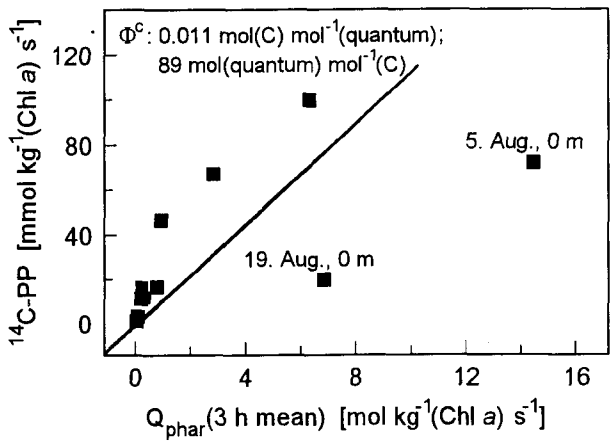

Fig. 6. ^{14}C primary production *versus* absorbed radiation (Q_{phar}) on four days in July and August. Q_{phar} values have been averaged over 3 h periods for incubation of phytoplankton in bottles.

Variation of Φ^C_{max} with photoacclimation and spectral variations in PAR distribution are not exceptional and have already been described in literature, especially for dinoflagellates (Prézelin *et al.* 1987, Kroon *et al.* 1993, Schofield *et al.* 1996). Very small values of Φ^C_{max} concerning the surface samples (0 m) can be an additional effect due to photoinhibition or the "bottle effect" (Fig. 4).

Table 6. Measured operational (Φ^C) and calculated maximum quantum yields (Φ^C_{max}) of carbon fixation [mol(C) mol^{-1}(quantum absorbed)] at various depths [m]. Φ^C was derived by dividing the measured ^{14}C-incorporation rate with the calculated Q_{phar} ($Q_{phar}1$) values (cf. Table 7). Φ^C_{max} was computed by means of Eq. (4). $\Phi^C_{max}{}^*$ and $\Phi^C_{max}{}^{**}$ represent calculations with 0.5 I_k and 2.0 I_k [µmol m^{-2} s^{-1}], respectively. $\bar{a}_{ph}$ [m^{-1}] is the spectrally-weighted absorption coefficient calculated according to Eq. (5). I_k is the saturation point of the the *P-I* curve derived from the fit with Eq. (3).

Date	Depth	$\bar{a}_{ph}$	I_k	Φ^C, measured	Φ^C_{max}, calculated	$\Phi^C_{max}{}^*$	$\Phi^C_{max}{}^{**}$
8 July	0	0.102	443.6	-	-	-	-
	1.0	0.053	392.8	0.071	0.079	0.086	0.075
	2.0	0.054	421.0	0.033	0.033	0.033	0.033
22 July	0	1.078	254.2	-	-	-	-
	0.5	0.731	259.7	0.035	0.046	0.057	0.041
	1.0	0.736	282.4	0.017	0.018	0.020	0.018
	2.0	0.417	272.5	0.072	0.073	0.074	0.073
19 August	0	0.727	313.0	0.003	0.011	0.019	0.007
	0.5	0.464	317.7	0.029	0.042	0.056	0.036
	1.0	0.376	302.8	0.057	0.065	0.073	0.061
	2.0	0.248	289.1	0.055	0.056	0.057	0.055

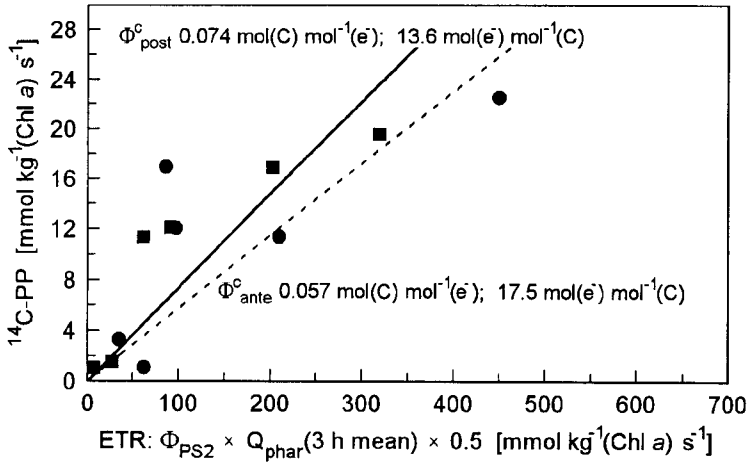

Fig. 7. ^{14}C primary production *versus* electron transport rates calculated with Φ_{PS2} before (*circles*, linear regression: *dashed line*) and after incubation (*squares*, linear regression: *solid line*) at different depths and days.

Oxygen evolution: The Q_{phar} values allow also to calculate theoretical oxygen production rates based on the PS2-related electron transport rates from PAM fluorescence measurements. Table 7 shows these theoretical oxygen evolution rates from 3 different days and for 3 differently computed Q_{phar} values. All PAR-saturated O_2 evolution rates were temperature-corrected depending on ΔT ($T_{in\ situ}$ - $T_{laboratory}$) by 8-37 % (values not shown). The results of the different Q_{phar} calculations are presented in Table 7. Uncorrected $Q_{phar}1$ decreased between 4-22 % compared to $Q_{phar}2$, when non-photosynthetic (photoprotective) pigments were subtracted from the overall reconstructed absorbance spectra ($Q_{phar}2$), depending on the Chl concentration and the fraction of PAR absorbed by phytoplankton. When correction is performed with the help of fluorescence excitation spectra from literature (Culver and Perry 1999), $Q_{phar}1$ decreases between 11-30 % compared to $Q_{phar}3$ with similar dependency on the fraction of PAR absorbed by phytoplankton. This dependency clearly shows that errors due to non-photosynthetic absorption of PAR are largest at low Chl concentrations and high irradiances. Therefore, a strong overestimation of theoretical O_2 evolution rates is most likely at the beginning or at the decline of a phytoplankton bloom. The ratio of absorbance to fluorescence excitation spectra of *Amphidinium carterae* (Culver and Perry 1999) was used to correct our reconstructed phytoplankton

Table 7. Incident irradiance Q_0 [µmol m^{-2} s^{-1}] at depth z, computed photosynthetically absorbed radiation Q_{phar} according to Eq. (2), and related oxygen evolution rates. $Q_{phar}1$ is computed without any correction of the reconstructed absorption spectra, $Q_{phar}2$ by subtracting the contribution of photoprotective pigments lutein, diadinoxanthin, alloxanthin, and zeaxanthin from the absorption spectra, and $Q_{phar}3$ by correcting the reconstructed absorbance spectra by means of literature based spectrally resolved ratios of absorption *versus* fluorescence excitation spectra (Culver and Perry 1999). Theoretically derived oxygen evolution rates as described in Materials and methods. O_2-Rate1, O_2-Rate2, and O_2-Rate3 [mmol kg^{-1}(Chl*a*) s^{-1}] were computed based on $Q_{phar}1$, $Q_{phar}2$, and $Q_{phar}3$ [µmol m^{-3} s^{-1}], respectively.

Date	Depth [m]	Q_0	$Q_{phar}1$	$Q_{phar}2$	$Q_{phar}3$	O_2-Rate1	O_2-Rate2	O_2-Rate3
8 July	0	608.00	58.80	45.72	40.37	305.17	237.29	209.52
	1.0	43.00	2.21	2.08	2.16	20.04	18.86	19.58
	2.0	1.74	0.09	0.09	0.09	0.84	0.84	0.84
22 July	0	942.00	621.31	595.87	558.60	75.34	72.25	67.73
	0.5	116.00	60.15	59.24	55.65	22.56	22.22	20.88
	1.0	34.00	17.71	17.60	17.66	7.10	7.06	7.08
	2.0	4.69	1.60	1.60	1.60	1.21	1.21	1.21
19 August	0	1161.00	599.86	562.24	500.64	146.36	137.18	122.15
	0.5	184.00	68.36	66.92	62.69	49.93	48.88	45.79
	1.0	52.00	16.28	16.17	16.19	14.80	14.70	14.72
	2.0	5.64	1.24	1.24	1.24	1.66	1.66	1.66

absorbance spectra. In the Bleiloch reservoir, diatoms and chlorophytes dominated the phytoplankton population. Culver and Perry (1999) reported for diatoms smaller ratios of absorbance to fluorescence excitation spectra than for dinoflagellates. These results were only presented in the form of averaged values without showing the spectral dependency, that is essential for our correction procedure, since the spectral radiation quality within the water column of the site 'Piere' changed dramatically with increasing depth. Hence, the correction of $Q_{phar}3$ is possibly too strong for the investigated type of phytoplankton as indicated by the maximum difference between $Q_{phar}2$ and $Q_{phar}3$ of 12 %.

Nevertheless, even after correction, the surface values (0 m) of O_2 evolution remained exceptionally high compared to those normally observed [50-80 mmol(O_2) kg^{-1}(Chl *a*) s^{-1}] (Table 7). Therefore, further factors reducing the theoretical O_2 evolution rates have to be taken into account.

The overestimation may originate from errors in the reconstruction of absorbance spectra from HPLC derived pigment concentrations due to the package effect (Geider and Osborne 1987). This has to be studied in detail in future for the water reservoir under investigation.

Physiological processes in the photosynthetic apparatus may also be the reason for this discrepancy: oxygen consuming reactions such as the pseudocyclic electron flow ("Mehler reaction") and photorespiration or non-oxygen consuming reactions such as cyclic electron flow around PS2 decrease the net O_2 evolution while the electrons transported through PS2 by these processes are detected in variable fluorescence measurements. Computing theoretical O_2 evolution rates from actual ETR measurements, therefore, results in an overestimation of O_2 evolution rates in comparison to actual O_2 evolution measurements. This can often be seen in a shift of fluorescence-based I_k to higher irradiances compared to that of oxygen-based *P-I* curves, provided that the measured and theoretically derived α-slopes of oxygen-based *P-I* curves are identical. This is the case, *e.g.*, for experiments with *Chlorella vulgaris* cells in our laboratory: Due to the additional electron flow in oxygen consuming reactions or cyclic electron transport around PS2 the saturation of ETR will be reached at higher irradiances compared to oxygen based measurements. Comparison of measured and theoretically derived oxygen *P-I* curves shows that at PAR-limited conditions the calculated O_2 rates are identical to O_2 rates actually measured, indicating that the above mentioned reactions do not play a significant role at low irradiances in overall electron transport. At saturating PAR, the theoretically derived O_2 rates are overestimated by a maximum of 30 % in comparison to the actual measured ones (M. Richter, personal communication). Oxygen consuming reactions might play a major role at high irradiances and hence would especially affect the O_2 evolution rates of surface samples. To test the influence of oxygen consuming reactions on theoretically derived O_2 evolution rates, F_v measurements can be performed in the presence of reduced oxygen concentrations (2 %), as already described in literature (Weis and Berry 1987, Genty *et al.* 1989). In such experiments linear relationships

between ETR and carbon fixation over the whole range of irradiances could only be obtained at strongly reduced oxygen concentrations.

In addition, there is a strong spectral dependency for the synthesis of different end-products in photosynthesis, well documented especially for green algae. In chlorophytes blue radiation and "white light" enhance the synthesis of amino acids and lipids over saccharides, requiring more ATP than the dominating synthesis of saccharides in red radiation (Brinkmann and Senger 1978). These processes will lead to an increased O_2/CO_2 ratio when higher amounts of ATP will be required than for the synthesis of saccharides.

Considering only all influencing factors on the basis of closely related PS2 ETR and oxygen release, one can imagine that derivation of carbon fixation rates from ETR measurements on a theoretical basis is even more complicated since not all electrons are transferred onto carbon but can also be translocated to other "sinks", such as synthesis of different storage compounds or nitrate and sulphate reduction.

Final conclusions: The present results show that the conversion of fluorescence based *P-I* curves of phytoplankton cells into *in situ* carbon fixation rates needs further research and must focus on the following problems:

1. It has to be tested how light scattering and the package effect of the cells influence the validity of the calculated fraction of absorbed PAR.
2. Due to the spectral variability of O_2/CO_2 ratios, oxygen and carbon have to be measured *in situ* simultaneously.
3. The physiological regulation of electron partitioning under PAR saturation has to be studied in detail to understand non-linear relationship between fluorescence and gas exchange based *P-I* curves.
4. Changes in physiological activity during bottle exposure have to be quantified in relation to the photosynthetic performance under natural conditions, especially under high Chl concentrations.

References

Baines, S.B., Pace, M.L.: The production of dissolved organic matter by phytoplankton and its importance to bacteria: Patterns across marine and freshwater systems. - Limnol. Oceanogr. **36**: 1078-1090, 1991.

Beutler, M., Meyer, B., Wiltshire, K.H., Moldaenke, C.: Differentiation of spectral groups of algae with computer-based analysis of fluorescence excitation spectra. - Vom Wasser **91**: 61-74, 1998.

Bidigare, R.R., Ondrusek, M.E., Morrow, J.H., Kiefer, D.A.: *In vivo* absorption properties of algal pigments. - SPIE **1302** (Ocean Optics X): 289-302, 1990.

Boyd, P.W., Aiken, J., Kolber, Z.: Comparison of radiocarbon and fluorescence based (pump and probe) measurements of phytoplankton photosynthetic characteristics in the Northeast Atlantic Ocean. - Mar. Ecol. Prog. Ser. **149**: 215-226, 1997.

Brinkmann, G., Senger, H.: The development of structure and function in chloroplasts of greening mutants of *Scenedesmus* IV. Blue light-dependent carbohydrate and protein metabolism. - Plant Cell Physiol. **19**: 1427-1437, 1978.

Cailliau, C., Claustre, H., Vidussi, F., Marie, D., Vaulot, D.: Carbon biomass, and gross rates as estimated from ^{14}C-pigment labelling, during photoacclimation in *Prochlorococcus* CCMP 1378. - Mar. Ecol. Prog. Ser. **145**: 209-221, 1996.

Culver, M.E., Perry, M.J.: The response of photosynthetic absorption coefficients to irradiance in culture and in tidally mixed estuarine waters. - Limnol. Oceanogr. **44**: 24-36, 1999.

Deutsche Einheitsverfahren zur Wasseruntersuchung nach EN ISO 9963-1 (C23). - VCH, Weinheim 1995.

Eilers, P.H.C, Peeters, J.C.H.: A model for the relationship between light intensity and the rate of photosynthesis in phytoplankton. - Ecol. Model. **42**: 199-215, 1988.

Falkowski, P.G., Wyman, K., Ley, A.C., Mauzerall, D.C.: Relationship of steady-state photosynthesis to fluorescence in eucaryotic algae. - Biochim. biophys. Acta **849**: 183-192, 1986.

Fitzwater, S.E., Knauer, G.A., Martin, J.H.: Metal contamination and its effect on primary production measurements. - Limnol. Oceanogr. **27**: 544-551, 1982.

Gallegos, C.L., Platt, T.: Photosynthesis measurements on natural populations of phytoplankton. - Can. Bull. Fish. aquat. Sci. **210**: 103-112, 1981.

Geel, C., Versluis, W., Snel, J.F.H.: Estimation of oxygen evolution by marine phytoplankton from measurement of the efficiency of Photosystem II electron flow. - Photosynth. Res. **51**: 61-70, 1997.

Geider, R.J., Osborne, B.A.: Light absorption by a marine diatom: experimental observations and theoretical calculations of the package effect in a small *Thalassiosira* species. - Mar. Biol. **96**: 299-308, 1987.

Genty, B., Briantais, J.-M., Baker, N.R.: The relationship between the quantum yield of photosynthetic electron transport and quenching of chlorophyll fluorescence. - Biochim. biophys. Acta **990**: 87-92, 1989.

Hartig, P., Coljin, F.: Pulse-amplitude-modulation fluorescence (PAM). A tool for fast assessment of primary productivity in the sea? - In: Dehairs, F., Goeyens, L., Bayens, J. (ed.): Integrated Marine System Analysis. Pp. 103-113. VUB Bruessel, Bruessel 1996.

Hartig, P., Wolfstein, K., Lippemeier, S., Coljin, F.: Photosynthetic activity of natural microphytobenthos

populations measured by fluorescence (PAM) and ^{14}C-tracer methods: a comparison. - Mar. Ecol. Prog. Ser. **166**: 53-62, 1998.

Hofstraat, J.W., Peeters, J.C.H., Snel, J.F.H., Geel, C.: Simple determination of photosynthetic efficiency and photoinhibition of *Dunaliella tertiolecta* by saturating pulse fluorescence measurements. - Mar. Ecol. Prog. Ser. **103**: 187-196, 1994.

Karl, D.M., Dale, V.H., Björkman, K., Letelier, R.M.: The role of dissolved organic matter release in the productivity of the oligotrophic North Pacific Ocean. - Limnol. Oceanogr. **43**: 1270-1286, 1998.

Kiefer, D.A., Mitchell, B.G.: A simple, steady state description of phytoplankton growth based on absorption cross section and quantum efficiency. - Limnol. Oceanogr. **28**: 770-776, 1983.

Kolber, Z., Falkowski, P.G.: Use of active fluorescence to estimate phytoplankton photosynthesis *in situ*. - Limnol. Oceanogr. **38**: 1646-1665, 1993.

Kolber, Z.S., Prášil, O., Falkowski, P.G.: Measurements of variable chlorophyll fluorescence using fast repetition rate techniques: defining methodology and experimental protocols. - Biochim. biophys. Acta **1367**: 88-106, 1998.

Kroon, B., Prézelin, B.B., Schofield, O.: Chromatic regulation of quantum yields for photosystem II charge separation, oxygen evolution, and carbon fixation in *Heterocapsa pygmaea* (*Pyrrophyta*). - J. Phycol. **29**: 453-462, 1993.

Lange, M., Guillou, L., Vaulot, D., Simon, N., Amann, R.I., Ludwig, W., Medlin, L.K.: Identification of the class prymnesiophyceae and the genus *Phaeocystis* with ribosomal RNA-targeted nucleic acid probes detected by flow cytometry. - J. Phycol. **32**: 858-868, 1996.

Li, W.K.W.: Estimation of primary production by flow cytometry. - ICES mar. Sci. Symp. **197**: 79-92, 1993.

Maestrini, S.Y., Sournia, A., Herbland, A.: Measuring phytoplankton production in 1992 and the coming years: a dilemma? - ICES mar. Sci. Symp. **197**: 244-259, 1993.

Moisan, T.A., Mitchell, B.G.: Photophysiological acclimation of *Phaeocystis antarctica* Karsten under light limitation. - Limnol. Oceanogr. **44**: 247-258, 1999.

Neale, P.J., Richerson, P.J.: Photoinhibition and the diurnal variation of phytoplankton photosynthesis - I. Development of a photosynthesis-irradiance model from studies of *in situ* responses. - J. Plankton Res. **9**: 167-193, 1987.

Nixdorf, B., Hoeg, S.: Phytoplankton - community structure, succession and chlorophyll content in Lake Müggelsee from 1979 to 1990. - Int. Rev. ges. Hydrobiol. **78**: 359-388, 1993.

Phinney, D.A., Cucci, T.L.: Flow cytometry and phytoplankton. - Cytometry **10**: 511-521, 1989.

Prézelin, B.B., Bidigare, R.R., Matlick, H.A., Putt, M., Ver Hoven, B.: Diurnal patterns of size-fractioned primary productivity across a coastal front. - Mar. Biol. **96**: 563-574, 1987.

Raven, J.A.: Implications of inorganic carbon utilization: ecology, evolution, and geochemistry. - Can. J. Bot. **69**: 908-924, 1991.

Rees, D., Lee, C.B., Gilmour, D.J., Horton, P.: Mechanisms for controlling balance between light input and utilisation in the salt tolerant alga *Dunaliella* C9AA. - Photosynth. Res. **32**: 181-191, 1992.

Schofield, O., Prézelin, B., Johnsen, G.: Wavelength dependency of the maximum quantum yield of carbon fixation for two red tide dinoflagellates, *Heterocapsa pygmaea* and *Prorocentrum minimum* (Pyrrophyta): Implications for measuring photosynthetic rates. - J. Phycol. **32**: 574-583, 1996.

Schofield, O., Prézelin, B.B., Smith, R.C., Stegmann, P.M., Nelson, N.B., Lewis, M.R., Baker, K.S.: Variability in spectral and nonspectral measurements of photosynthetic light utilization efficiencies. - Mar. Ecol. Prog. Ser. **78**: 253-271, 1991

Schreiber, U.: New emitter-detector-cuvette assembly for measuring modulated chlorophyll fluorescence of highly diluted suspensions in conjunction with the standard PAM fluorometer. - Z. Naturforsch. **49c**: 646-656, 1994.

Schreiber, U., Endo, T., Mi, H., Asada, K.: Quenching analysis of chlorophyll fluorescence by the saturation pulse method: Particular aspects relating to the study of eukaryotic algae and cyanobacteria. - Plant Cell Physiol. **36**: 873-882, 1995a.

Schreiber, U., Hormann, H., Neubauer, C., Klughammer, C.: Assessment of photosystem II photochemical quantum yield by chlorophyll fluorescence quenching analysis. - Aust. J. Plant Physiol. **22**: 209-220, 1995b.

Schreiber, U., Neubauer, C., Schliwa, U.: PAM fluorometer based on medium-frequency pulsed Xe-flash measuring light: A highly sensitive new tool in basic and applied photosynthesis research. - Photosynth. Res. **36**: 65-72, 1993.

Sharp, J.H.: Excretion of organic matter by marine phytoplankton: do healthy cells do it? - Limnol. Oceanogr. **22**: 381-399, 1977.

Smith, R.C., Prézelin, B.B., Bidigare, R.R., Baker, K.S.: Bio-optical modeling of photosynthetic production in coastal waters. - Limnol. Oceanogr. **34**: 1524-1544, 1989.

Trtilek, M., Kramer, D.M., Koblizek, M., Nedbal, L.: Dual-modulation LED kinetic fluorometer. - J. Lumin. **72-74**: 597-599, 1997.

van Kooten, O., Snel, J.F.H.: The use of chlorophyll fluorescence nomenclature in plant stress physiology. - Photosynth. Res. **25**: 147-150, 1990.

Walsby, A.E.: Numerical integration of phytoplankton photosynthesis through time and depth in a water column. - New Phytol. **136**: 189-209, 1997.

Watanabe, Y.: A study of the excretion and extracellular products of natural phytoplankton in Lake Nakanuma, Japan. - Int. Rev. ges. Hydrobiol. **65**: 809-834, 1980.

Weis, E., Berry, J.A.: Quantum efficiency of Photosystem II in relation to "energy"-dependent quenching of chlorophyll fluorescence. - Biochim. biophys. Acta **894**: 198-208, 1987.

Wilhelm, C., Lohmann, C.: Recent progress in the identification and determination of freshwater phytoplankton in the natural environment. - In: Sutcliffe, D.W. (ed.): The Microbiological Quality of Water. Pp. 81-91. Freshwater Biological Associations Special Publications, Ambleside 1997.

Wilhelm, C., Volkmar, P., Lohmann, C., Becker, A., Meyer, M.: The HPLC-aided pigment analysis of phytoplankton cells as a powerful tool in water quality control. - J. Water SRT - Aqua (London) **44**: 132-141, 1995.

Wilhelm, C., Wild, A.: The variability of the photosynthetic unit in *Chlorella*. II. The effect of light intensity and cell

development on photosynthesis, P-700 and cytochrome *f* in homo-continuous and synchronous cultures of *Chlorella*. - J. Plant Physiol. **115**: 125-135, 1984.

Williams, P.J.L., Jenkinson, N.W.: A transportable microprocessor-controlled precise Winkler titration suitable for field station and shipboard use. - Limnol. Oceanogr. **27**: 576-584, 1982.

Williams, P.J.L., Robertson, J.I.: A serious inhibition problem from a Kinskin sampler during phytoplankton productivity studies. - Limnol. Oceanogr. **34**: 1300-1305, 1989.

Yentsch, C.S., Phinney, D.A.: Spectral fluorescence: An ataxonomic tool for studying the structure of phytoplankton populations. - J. Plankton Res. **7**: 617-632, 1985.